Synthesis of Carbon Dots with Multiple Color Emission by Controlled Graphitization and Surface Functionalization

Xiang Miao, Dan Qu, Dongxue Yang, Bing Nie, Yikang Zhao, Hongyou Fan, and Zaicheng Sun**

Multiple-color-emissive carbon dots (CDots) have potential applications in various fields such as bioimaging, light-emitting devices, and photocatalysis. The majority of the current CDots to date exhibit excitation-wavelength-dependent emissions with their maximum emission limited at the blue-light region. Here, a synthesis of multiple-color-emission CDots by controlled graphitization and surface function is reported. The CDots are synthesized through controlled thermal pyrolysis of citric acid and urea. By regulating the thermal-pyrolysis temperature and ratio of reactants, the maximum emission of the resulting CDots gradually shifts from blue to red light, covering the entire light spectrum. Specifically, the emission position of the CDots can be tuned from 430 to 630 nm through controlling the extent of graphitization and the amount of surface functional groups, —COOH. The relative photoluminescence quantum yields of the CDots with blue, green, and red emission reach up to 52.6%, 35.1%, and 12.9%, respectively. Furthermore, it is demonstrated that the CDots can be uniformly dispersed into epoxy resins and be fabricated as transparent CDots/epoxy composites for multiple-color- and white-light-emitting devices. This research opens a door for developing low-cost CDots as alternative phosphors for light-emitting devices.

X. Miao, Dr. D. Qu, D. Yang, B. Nie, Y. Zhao, Prof. Z. Sun
Beijing Key Lab for Green Catalysis and Separation
Department of Chemistry and Chemical Engineering
College of Environmental and Energy Engineering
Beijing University of Technology
100 Pingleyuan, Beijing 100124, P. R. China
E-mail: sunzc@bjut.edu.cn

X. Miao
State Key Laboratory of Luminescence and Applications
Changchun Institute of Optics
Fine Mechanics and Physics
Changchun 130033, Jilin, P. R. China

X. Miao
Graduate School
University of Chinese Academy of Sciences
Beijing 100049, P. R. China

B. Nie, Y. Zhao
Beijing Guangqumen High School
Dongcheng District, Beijing 100000, P. R. China

Prof. H. Fan
Sandia National Labs
1001 University Blvd., Albuquerque, NM 87106, USA
E-mail: hfan@sandia.gov

The ORCID identification number(s) for the author(s) of this article can be found under https://doi.org/10.1002/adma.201704740.

DOI: 10.1002/adma.201704740

As a new member of the carbon material family, carbon dots (CDots) endow carbon materials with luminescent property and expand their application in fluorescent field. Because of their unique optical property, they have attracted much more attention for their potential applications in the photoelectrical conversion,[1] photocatalysis,[2] bioimaging systems,[3] and light-emittaing devices (LEDs)[4] since CDots were discovered in 2004.[5] In early research, CDots had low photoluminescence (PL) quantum yield (QY) and the emission was limited at blue light emission. Over a decade, researchers have put much more effort to improve their PL QY through surface passivation and heteroatom doping methods to induce better charge/carrier transport. Since then, the PL QY of CDots can reach up to 94% for strong blue emission[6] and ≈60% for green emission.[7] This progress leads to potential applications for CDots in bioimaging, optoelectronic devices, and LEDs due to their low toxicity, biocompatibility, and excellent photostability.[3e,8] However, efficient red emissive CDots are still highly desired because red light has deep tissue penetration for bioimaging and is one of the primary colors for white LEDs. There are a few reports on the synthesis of red emissive CDots. For example, using expensive polythiophene phenylpropionic acid as a precursor, Wang and co-workers developed hydrothermal reaction processes to prepare red emissive CDots with low PL QY of 2.3%.[9] Our group reported synthesis of red emissive CDots with 8% PL QY using citric acid (CA) and thiourea, which results in S- and N-doped CDots with enhanced electron delocalization.[10] Lin and co-workers demonstrated synthesis of red emissive CDots with PL QY of 26%. The CDots were prepared through solvothermal route using phenylenediamine isomers.[11] Xiong and co-workers reported the red-emitting CDots with PL QY of ≈24%. The red emission was achieved by tuning the surface state from precursors p-phenylenediamine and urea that were prepared carefully through silica column chromatography.[12] Recently, Yang's group used dopamine and *o*-phenylenediamine as precursors and obtained near infrared emissive CDots by generating large sp^2 domains. The final QY of the CDots can reach to ≈30%.[13] Despite these efforts, the final materials are expensive for practical applications and lack of clear understanding of luminescence mechanism. Thus,

simple and facile synthesis route is still highly desirable.

CDots can be treated as a conjugated graphite core with functional groups on the surface. Theoretical calculations and experimental results have shown that the energy gap of π–π^* (or band gap) strongly depends on the effective conjugation length or sp^2 domain size.[14] In addition, it has been shown that surface functional groups also have critical effect on the red shift of emission.[12,13,14b] Here we developed a synthesis strategy to prepare multiple color emissive CDots by tuning the effective conjugation length and amount of surface functional groups. The CDots are synthesized through controlled thermal pyrolysis of CA and urea. By regulating the thermal pyrolysis temperature, the maximum emission of the resulted CDots gradually shifts from blue to red light, covering the entire light spectrum. Specifically, the emission position of CDots can be tuned from 430 to 630 nm through controlling the extent of graphitization and the amount of surface function groups —COOH. The relative photoluminescence quantum yields of the CDots with blue, green, and red emission reach up to 52.6%, 35.1%, and 12.9%, respectively. To our best knowledge, this is the first demonstration for preparation of highly efficient multiple color emissive CDots from same precursors in a single step. The CDots can be dissolved in various polar organic solvents such as alcohol, dimethylformide (DMF), dimethylsulfone (DMSO), dioxane, and amine. We further fabricate the CDots/epoxy composites by dissolving CDots into the tetraethylpentaamine (TEPA) as hardener of epoxy resins. The CDots/epoxy can be used as blue, green, and red phosphors and encapsulation materials for multiple color LED. By mixing controlled amount of blue, green, and red CDots into epoxy resins, we fabricated pure white LED with Commission on Illumination (CIE) coordinate (0.33, 0.34), correlated color temperature (CCT) of 5606 K and color rendering index (CRI) of 92. This report provides a general synthesis route to produce tunable color emissive CDots from common CA and urea, which is beyond the previous reports that red emissive CDots are produced from aromatic compounds. We also demonstrate its application in phosphor-based LEDs. Actually, they also potentially apply to the fields of photoelectron conversion, bioimaging, and ion or molecular sensing due to their broad absorption, long wavelength excitation, and multiple surface functional groups.

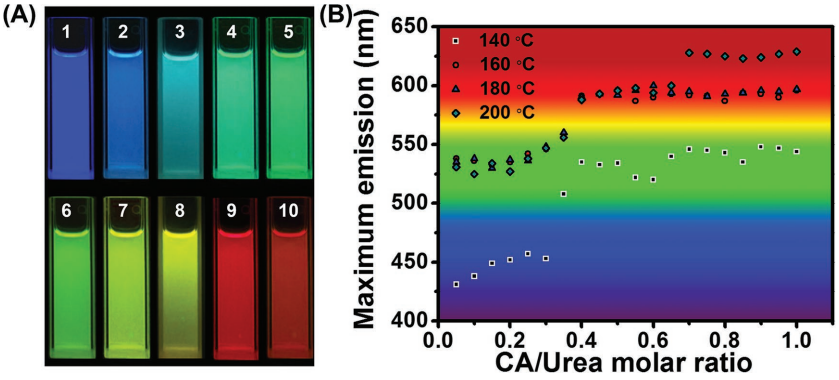

Figure 1. Optical property of the CDots ethanol solution prepared from CA and urea at different reaction conditions. A) Optical images of luminescence CDots prepared from different reaction conditions (for the detailed reaction conditions see Table S1 in the Supporting Information) under different excitation light. B) The maximum emission peaks of CDots at different molar ratios of CA to urea and different reaction temperatures.

Multiple color emissive CDots were prepared using CA and urea in DMF with controlled molar ratio of CA to urea in the range of 0–1.0. The reaction temperature was controlled from 140 to 200 °C to control the extent of graphitization. Typically, 7.5 mmol CA and 10 mmol urea was dissolved into 10 mL DMF solution. To synthesize red emissive CDots, the solution was kept at 200 °C for 12 h in a 20 mL Teflon-lined stainless-steel autoclave. The CDots were collected by centrifuging the red solution at 10 000 rpm for 10 min. The supernatant was added into the mixed solvents of petroleum ether and ethyl acetate to remove unreacted molecules and then the solid was dried at 70 °C overnight. **Figure 1**A shows the optical images of CDots prepared from different reaction conditions in ethanol solution under different excitation light. They emit different colors covering from blue to red indicating that the emission of CDots can be tuned by reaction condition. Figure 1B shows that the maximum emission peaks of the CDots vary with the reaction conditions such as the ratios of CA/urea and reaction temperatures. From Figure 1B it can be seen clearly that there exists a magic transition region at CA/urea = 0.3–0.4, where the maximum emissions of CDots has been dramatically shifted to red. This indicates that the high molar ratio of CA/urea leads to the red shift of CDots emission because of high extent of carbonization in the materials. When the reaction temperature is 140 °C, the maximum emission peaks change from blue (≈425 nm) at low molar ratio of CA/urea to green (≈530 nm) at high molar ratio of CA/urea. When the reaction temperature is increased to 160 °C and above, the CDots display green emission (≈540 nm) at low molar ratios of CA/urea. It is further shifted to red emission (≈600 nm) when the molar ratio of CA/urea is higher than 0.3. Furthermore, the maximum emission peak can be shifted to red spectrum region (≈630 nm) when the reaction temperature is set at 200 °C and the molar ratio of CA/urea is larger than 0.7. As it is known, higher temperature will promote the graphitization of CA. On the basis of above results, we conclude that the emission of CDots strongly depends on the graphitization degree of CA. Figure S1 of the Supporting Information exhibits the color coordinates (x, y) calculated from corresponding PL emission spectra on the CIE 1931 color space. All the points cover blue, green, and red light regions, indicating that the emission of CDots can be continuously tuned by changing reaction conditions.

To understand the effect of reaction conditions on the PL emission of the CDots, three typical CDots are chosen as model samples for further investigation. According to their emissive colors, they were denoted as B-CDots, G-CDots, and R-CDots, respectively. They were prepared at conditions: CA/urea = 0.1 at 140 °C for B-CDots, CA/urea = 0.3 at 160 °C for G-CDots and CA/urea = 0.75 at 200 °C for R-CDots, respectively. **Figure 2**A–C shows the transmission electron microscopy (TEM) images of B-CDots, G-CDots, and R-CDots, respectively. The three CDots possess very similar particle size. The average particle sizes

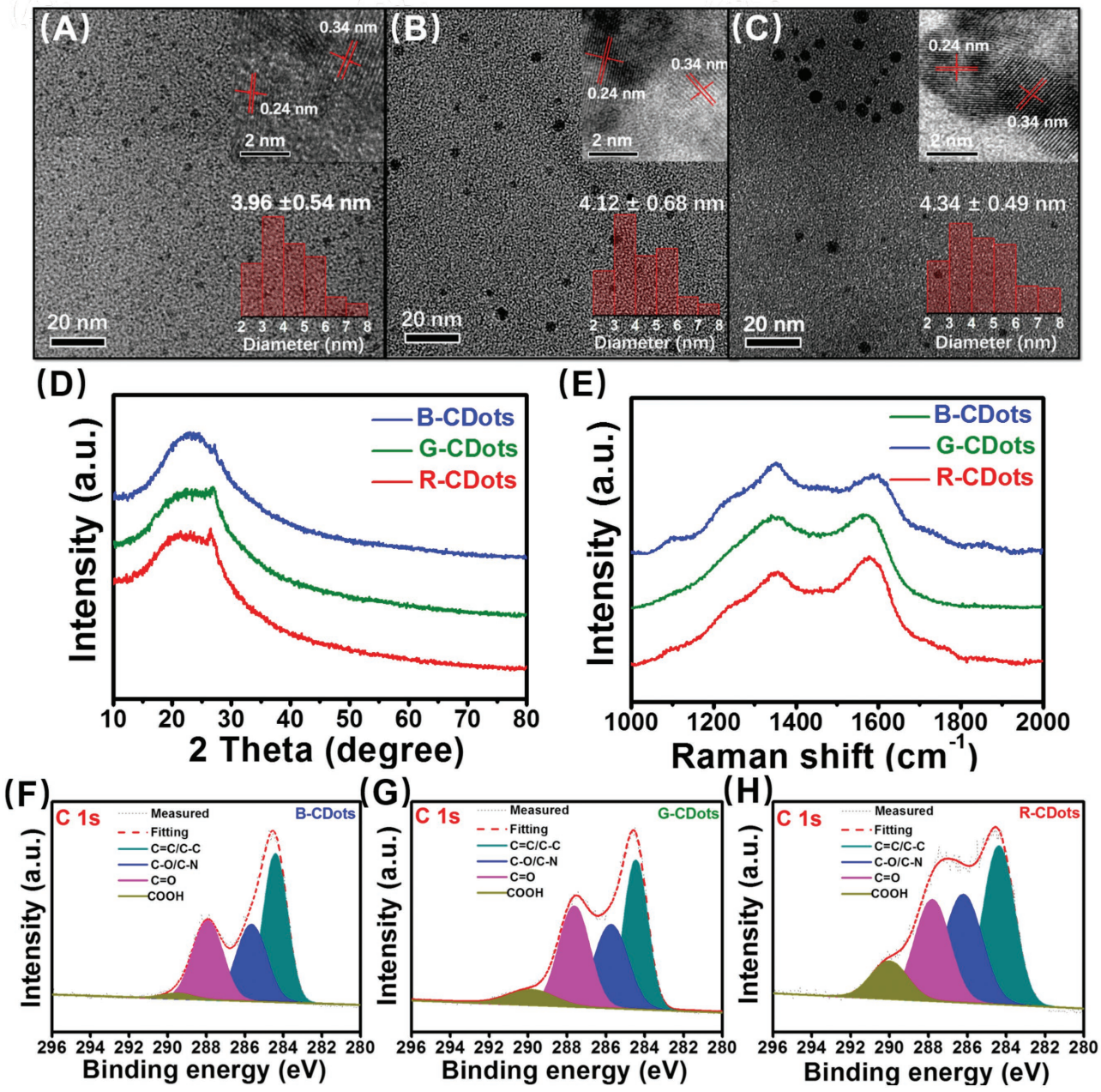

Figure 2. Morphologies and structural characterization of the CDots. A–C) TEM images of B-CDots (A), G-CDots (B), and R-CDots (C). Insets are the corresponding high resolution TEM at top right corner and particles size distributions at bottom right corner. D) XRD patterns of the three typical CDots. E) Raman spectra of the three typical CDots. F–H) The high-resolution C1s XPS spectra of B-CDots (F), G-CDots (G), and R-CDots (H), respectively.

are 3.96 ± 0.54, 4.12 ± 0.68, and 4.34 ± 0.49 nm for B-CDots, G-CDots, and R-CDots, respectively. The HR TEM images illustrate that all these three CDots have highly crystalline carbon structure. Two types of lattice fringe distance were observed at 0.24 and 0.34 nm that are attributed to the *d* spacings of the graphene (100) and graphite (001) planes.

X-ray diffraction patterns (XRD), as shown in **Figure 3**D, exhibit a broad peak at 21° and a minor sharp peak at 26.6°, which are attributed to the graphitic structure with interlayer spacing (002) of 0.41 and 0.34 nm. The broad peak at 21° large, corresponding to *d* spacing of 0.41 nm is contributed from enlarged interlayer distance, resulting from steric hindrance of functional groups on the graphene edge or the plan distortion from sp^3 C in the graphene plan. The peak at 26.6° is the characteristic (002) diffraction peak of graphite. Its appearance indicates the interlayer stacking within CDots is very close to that in graphite (≈0.35 nm). That indicates that close packing (0.35 nm) of highly conjugate sp^2 domain takes dominant place within the core part of CDots. On the edge of CDots, the functional groups or sp^3 C will enlarge the interlayer distance. Because the red emissive CDots has the strongest peak at 26.6°, which suggests that the R-CDots possess high extent of graphitization. In other

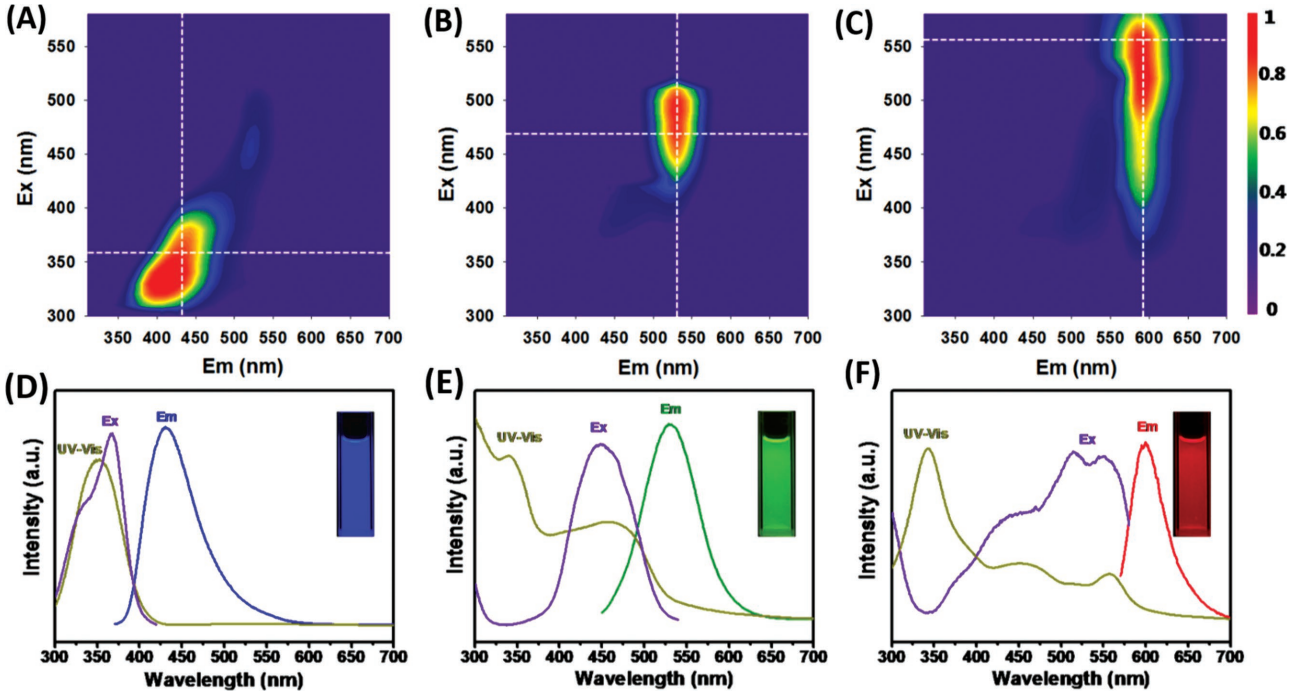

Figure 3. Optical properties of the three typical CDots with blue, green, and red emissions. A–C) Excitation–emission matrix for B-CDots (A), G-CDots (B), and R-CDots (C). D–F) The corresponding UV–vis, PL emission, and PL excitation spectra of B-CDots (D), G-CDots (E), and R-CDots (F).

words, R-CDots possess larger effective conjugation length than B- and G-CDots. Figure 2E shows typical Raman spectra of the three CDots. It exhibits two peaks at 1354 and 1581 cm^{-1} that correspond to the disordered (D band) and graphite (G band) of carbon materials. As it is known, the ratio of I_D/I_G is characteristic of the extents of graphite and the ratio of sp^3/sp^2 carbon. The ratio of I_D/I_G is 1.16, 0.97, and 0.89 for B-CDots, G-CDots, and R-CDots, respectively. The decrease ratio value implies the increasing graphite content in the CDots from B-, G- to R-CDots, indicating that the graphitization of CDots is enhanced in red emissive CDots which was prepared at the higher molar ratios of CA/urea and higher reaction temperature.

To further understand the role of functional groups, various spectroscopy characterizations were employed to investigate the structure of CDots. Figure S2 of the Supporting Information shows the Fourier transform infrared (FT-IR) spectra of CDots. The stretching vibration for OH (3436 cm^{-1}), NH (3190 cm^{-1}), CH_2 (2934 cm^{-1}), C=C (1617 cm^{-1}), C=N (1662 cm^{-1}), and C=O (1727 cm^{-1}) indicate the presence of conjugated aromatic structure together with O- and N-containing groups. To investigate the composition and valance state of CDots, X-ray photoelectron spectroscopy (XPS) was employed to characterize the surface group of the three typical CDots. Figure S3 of the Supporting Information shows the full survey of XPS of all three CDots, which are composed of C, O, and N elements. The ratio of N to C changes from 0.436, 0.369 to 0.330, respectively, indicating the increasing of carbon content. The O to C ratio increases from 0.165, 0.291 to 0.378 for B-CD, G-CDots, and R-CDots, respectively, indicating the increase of oxygen content. Figure 3D–F illustrates the high resolution C1s XPS spectra of all three CDots. The C1s spectra can be fitted into 4 kinds of C species sp^2 C (C=C/C−C) at 284.4 eV, sp^3 C (C−O and C−N) at 285.7 eV, −C=O at 287.9 eV and −COOH at 290.1 eV. It clearly shows the content of −COOH group significant increases from B-, G-, to R-CDots. The N1s and O1S high resolution XPS spectra are shown in Figure S4 (Supporting Information). For N1s, XPS spectra can be converted into pyridinic N (399.2 eV), pyrollic N (400.5 eV), and graphitic N (401.8 eV), respectively. The relative content of graphitic N decreases from B-, G- to R-CDots. The pyridinic N and pyrrolic N have similar relative amount. The high resolution XPS spectra of O1s contains two components associated with C−O at 534 eV and C=O at 531.7 eV. The relative amount of C=O slightly increases.

According to Chen and co-workers' theoretical calculation,[12] the emission wavelength of ideal graphene quantum dots (GQD) strongly depends on the size of GQD. The emission wavelength of GQD shifts from 235.2 nm for the smallest GQD (benzene) to 999.5 nm for 2.31 nm GQD (Figure S5, Supporting Information). The emission wavelength is a linear relationship with the size of GQD. The red shift of the emission wavelength with increasing size is because of the decrease in band gap resulting from π electron delocalization within the sp^2 domain. In the theoretical calculation, the size of GQD is equal to the effective conjugation length or graphitization. In our cases, although the size of CDots slightly increase from 3.96 to 4.34 nm in TEM images, the graphitization degree of CDots shows different base on the results of XRD and Raman in our cases. The high extent of graphitization in R-CDots stands for the extended effective conjugation length or large sp^2 domain. Consequently, the CDots with high graphitization degree have red-shift emission wavelength. In addition, they also calculated the emission wavelength of oxidized GQD as function of the coverage of −OH and/or −COOH group. Attaching both −OH and −COOH groups to the GQD continuously change GQD

emission from green (572.4 nm) to red (732.3 nm for −OH and 612.3 nm for −COOH, Figure S6, Supporting Information). In this report, the amount of −COOH group is clearly increased from B-, G- to R-CDots based on XPS results. The increase of −COOH content in CDots also results in red shift of emission, which is agreed with previous report.[12] On the basis of the above results, the red shift of CDots emission is contributed from both the increase in the extent of graphitization in CDots and more −COOH groups on the surface of CDots.

Figure 3 shows the optical characterization results of B-CDots, G-CDots, and R-CDots. For B-CDots, the maximum emissions gradually shift from 380 to 480 nm when the excitation wavelength changes from 320 to 400 nm (Figure 3A), indicating that B-CDots exhibit excitation dependent emission properties. Trace amount of green emissive CDots with the emission at ≈530 nm was observed. Red emission was not found implying there are no red emissive CDots in B-CDots. In the case of G-CDots, the emission peaks mainly are from ≈540 nm within the excitation wavelength from 420 to 520 nm (Figure 3B), indicating that it is excitation independent emission. For R-CDots, there is a long emission range with a maximum peak at ≈600 nm within the range of excitation wavelength from 400 to 575 nm regardless of excitation wavelength indicating that R-CDots have excitation independent emission (Figure 3C). Both blue and green light emissions are relatively weak even under short excitation wavelength. These results suggest that the emission of CDots prepared by this method can be customized by reaction conditions. Figure 3D–F shows the results of UV–vis spectra, PL emission, and PL excitation spectra taken along the horizontal and vertical dash line in the corresponding excitation–emission matrix in Figure 3A–C. B-CDots exhibit a strong absorption band at 350 nm, which is usually assigned to the n–π^* transition of conjugated C=O and C=N.[15] The emission of B-CDots is at ≈440 nm with excitation wavelength of 360 nm. The photoluminescence excitation (PLE) spectrum of 440 nm emission is close to the absorption band at 350 nm, indicating that the emission is originated from the n–π^* transition of conjugated C=O and C=N. In the case of G-CDots, another absorbance band was observed at 470 nm besides the absorbance band at 350 nm. The PLE spectrum of emission at 550 nm covers the band at 470 nm implying the green light emission is originated from the transition of absorption band at 470 nm, not related to the band at 350 nm. In other words, UV light cannot excite the green emission. Two more absorption peaks appear at 520 and 550 nm in the R-CDots. These new peaks are attributed to n–π^* transitions of the aromatic sp^2 system containing C=O and C=N bonds, respectively.[16] The PLE spectrum of emission at ≈600 nm covers the three transition band from 400 to 550 nm. Similarly, UV light cannot excite the red emission either. The relative PL QY of CDots were calculated to be 52.6% for B-CDots, 35.1% for G-CDots, and 12.9% for R-CDots using quinine sulfate, fluorescein isothiocyanate, and Rhodamine B as the references, respectively. The PL excitation spectra of CDots indicate that the emission mainly contributes from the absorption bands from the n–π^* transition of aromatic sp^2 system containing C=O and C=N bonds.

We found that the as-prepared CDots are well dissolved in various polar organic solvents such as alcohol, DMF, DMSO, dioxane, and amine, but are hard to be dispersed in nonpolar organic solvents. A few research groups have fabricated CDots/polymer composites using water-soluble polymers such as poly(acrylic acid) (PAA), poly(vinyl alcohol) (PVA), starch, and poly(vinylpyrrolidone) (PVP) for solid lighting devices or detectors.[10a,14c,17] In our case, the as-prepared CDots can be well dispersed in various polar organic solvents such as ethanol, DMSO, DMF, ethylenediamine (Figure S7, Supporting Information). They form transparent solutions indicating CDots are well dissolved in the solvents. The solutions exhibit different color emissions under different irradiation wavelength. The PL emission spectra of CDots in various solvents (Figures S8 and S9, Supporting Information) exhibit very little changes (within the range of 30 nm) in the maximum emission peak. Since all these solutions maintain the original optical properties of CDots indicating that no aggregation happens in these solvents, it provides opportunity to fabricate CDots/polymer composites through solution process method. Figure S10 of the Supporting Information exhibits optical and fluorescent images of CDots/polymer composites, polymer can be PVP, poly(ethylene oxide), poly(methyl methacrylate), and others. Epoxy resin is a common thermoset resin for paints, adhesives, sealant for electronic industry. For example, epoxy resin is extensively employed for encapsulation of the LED chips. If the phosphors can be uniformly dispersed into the epoxy resin, the epoxy resin will be endowed with phosphor function. We dissolved the CDots first in the epoxy hardener part (TEPA, 2 μg mL^{-1}) to form a clear solution. The epoxy solution was then mixed with hardener with 3:1 volume ratio. Finally, the mixture was left over 4 h at room temperature for curing to achieve the CDots/epoxy composites. **Figure 4**A,B shows the optical micrographs of CDots/epoxy composite discs with about 2 cm in diameter and 3–5 mm in thickness. After curing, the epoxy discs display different colors due to the different kinds of added CDots. All these epoxy discs are transparent and exhibit uniform multiple color emissions from blue to red under corresponding excitation light. Typically, CDots/epoxy composite discs show strong emissions with PL QY of 38.6%, 29.8%, and 7.4% for blue, green, and red emission (Table S2, Supporting Information), respectively. The PL emission spectra of CDots/epoxy composite discs are shown in Figure S11 (Supporting Information). The emission peak positions of composites are same as those from the CDots solutions, which further confirms the CDots are well dispersed into the epoxy matrix (Figure 2). These results suggest that there is no change of chemical structure and no aggregation in CDots/epoxy composites in comparison with the corresponding solutions. The CDots/epoxy composites were also applied to encapsulate LED chips. Figure 4C shows the optical images of the monochrome blue, green, and red down-conversion LED devices by coating CDots/epoxy on the different chips (chip emission at 365, 450, and 530 nm). The corresponding spectra of light emission are shown in Figure 4D. The emission bands locate at ≈440, ≈540, and ≈620 nm, respectively, for the blue, green, and red LED. The spectra of LED device are same as that of corresponding CDots solutions indicating that CDots are well dispersed in the epoxy resins for application of phosphor and encapsulation materials.

To fabricate the white LEDs, B-, G-, and R-CDots are mixed together into the epoxy hardener portion followed by mixing with epoxy portion in 1:3 volume ratio for encapsulation of UV-chip (365 nm). By varying the weight ratios of three kinds of CDots (Figures S12 and S13, Supporting Information), the

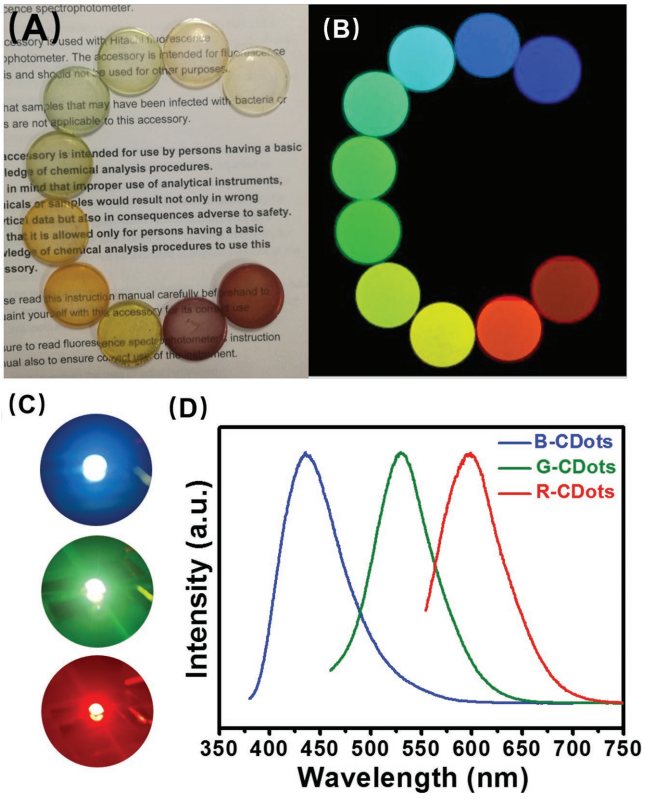

Figure 4. Optical properties of CDots/epoxy composites and corresponding LED devices. The optical photographs of the CDots/epoxy composite discs under A) room light and B) different excitation light. C) The photographs of the monochrome blue, green, and red down-conversion LED devices by coating CDots/epoxy on the different chips. D) The light emission spectra of LED devices in (C).

emission spectra of white LEDs can be tuned to pure white light when the weight ratio of CDots in epoxy composite is 1:3:2. The CIE color coordinates of white LEDs is (0.33, 0.34) in white light region (**Figure 5**A). The CCT and CRI of the white LEDs are 5606 K and 92, respectively. This light is very close to the natural sun light. The emitting light spectrum is shown in Figure 5B, which covers most of the visible-light region from 400 to 670 nm. To test the stability of the white LED device, the device is kept continuously illustrating over 20 d. The emitting light spectra of the white LED device at the beginning of and after 20 d are shown in the Figure 5C. The emitting light spectrum has insignificant change compared with most organic dyes of which the intensity is less than 80% after exposure of UV light for only 1 min.[6] This indicates that the CDots based white LED device has excellent stability. There is no photo bleach for CDots based white LED devices. These further confirm the stability of the CDots as potential phosphors for LEDs.

In summary, we developed new synthesis of CDots through thermal pyrolysis of CA and urea. We demonstrated the emission of the CDots can be tuned by controlling the reaction conditions such as increasing the ratios of CA/urea and reaction temperature. The emissions are shifted from blue to red in the case of increasing effective conjugation length and the amount of surface functional groups, such as −COOH. The as-prepared CDots are very well dissolved in the polar organic solvents to form homogenous solutions that maintain strong light emissions. We further demonstrated the facile preparation of CDots/polymer composite discs using these CDot solutions. Epoxy was used as matrix for fabrication of CDots/epoxy resin discs that exhibit the same light emissive properties as in solutions. We have shown that these CDots resin discs can be fabricated as efficient phosphor-based LED devices with different color light emissions. By mixing three types of CDots into epoxy resins,

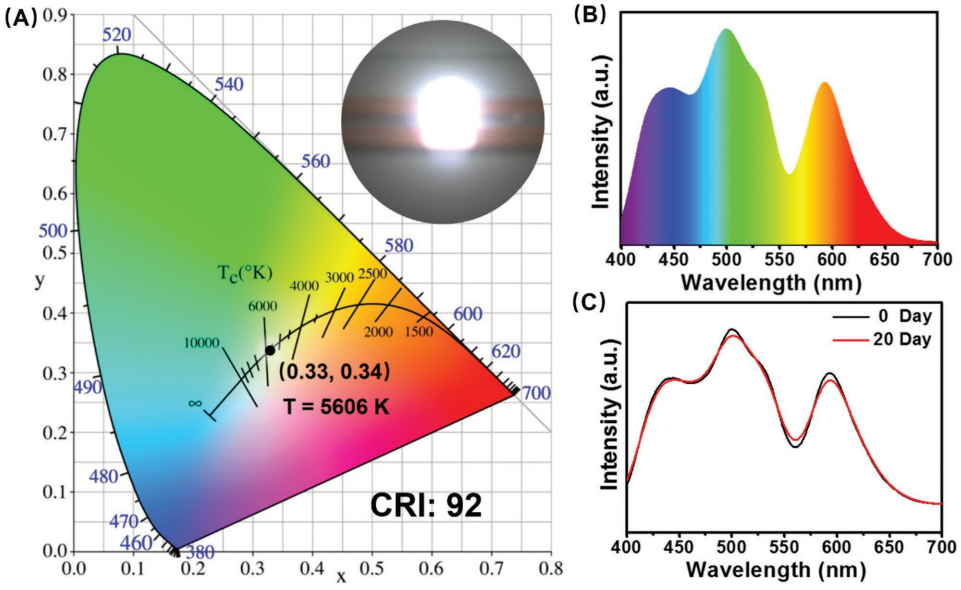

Figure 5. Characterization of white LED fabricated using the CDots. A) The CIE color coordinates of the white LEDs. Inset at right top corner is the optical photograph of the white LED at on-state. B) The emitting light spectrum of white LEDs. C) The emitting spectra of the white LED at initial and after illustrating over 20 d.

pure white LED devices were achieved with color coordination of (0.33, 0.34) and CRI of 92. The white LED devices exhibit excellent stability and no photo bleach was observed.

Experimental Section

Synthesis and Characterizations of CDots: Multiple color emissive CDots were synthesized by using different molar ratios of CA to urea in DMF at different temperatures. Typically, 1 mmol CA and 10 mmol urea were dissolved in 10 mL DMF for synthesis of blue emissive CDots. The mixture was then transferred into 20 mL Teflon-lined stainless-steel autoclave, heated to 140 °C, and kept for 12 h. The reaction solution was centrifuged at 10 000 rpm for 10 min to remove the solid. The supernatant was collected and added into the mixed solvent of petroleum ether and ethyl to obtain the solid. The ratio of petroleum and ethyl acetate varies with different CDots. Generally, the ratio of petroleum ether and ethyl acetate is 1:1 for blue emissive CDots; 3:1 for green emissive CDots; and 4:1 for red emissive CDots, respectively. By adjusting the ratios of CA to urea and the temperature of reaction, CDots with different emissive colors can be synthesized. At the ratio of CA to urea = 0.05–0.3 and the temperature at 140 °C, the blue emissive CDots were obtained; at the ratio of CA to urea = 0.3–1.0 and the temperature at 140 °C and the ratio of CA to urea = 0.05–0.3 and the temperature from 160 to 200 °C, the green emissive CDots were obtained; at the ratio of CA to urea = 0.3–1.0 and temperature from 160 to 200 °C, the red emissive CDots were obtained.

Preparation of the CDots/Epoxy Composites: A certain amount of CDots were dissolved in TEPA, then triple amount of epoxy was added into the mixture. The mixture was stirred to form a homogeneous mixture. The mixture was then put into the mold and maintained for 4 h at room temperature for curing. Typically, 5 μg B-CDots were dissolved in 50 μL TEPA to form the homogeneous solution. 150 μL epoxy was then added into the solution with stirring. After 4 h curing, the blue emissive CDots/epoxy composite was obtained.

Preparation of the LED Devices: The mixture of CDots and epoxy was drop-casted on the LED chip carefully, and cured at room temperature for 4 h. For the white LED, 1 μg B-CDots, 3 μg G-CDots, and 2 μg R-CDots were mixed with 50 μL TEPA and 150 μL epoxy, and then the homogeneous mixture was drop-casted on the LED chip (365 nm). For the blue LED, 5 μg B-CDots mixture was used to form epoxy composite and drop-casted on the LED chip (365 nm). Similarly, 5 μg G-CDots epoxy composite solution was casted on the LED chip (450 nm) for the green LED. 5 μg R-CDots and LED chip (530 nm) were used for the red LED.

Material Characterizations: Ultraviolet–visible absorption spectra were recorded using Shimadzu UV-2600 spectrophotometer. PL spectra were collected on the HITACHI F-7000 fluorescence Spectrophotometer. High-resolution TEM images were obtained with a JEOL JEM-1011 transmission electron microscope. FT-IR spectra were collected by a Bruker Vertex 70 spectrometer. XPS were obtained on a Thermo Scientific ESCALAB 250 Multi-technique Surface Analysis. Raman spectra were collected on Lab RAM HR Raman microscope.

Supporting Information

Supporting Information is available from the Wiley Online Library or from the author.

Acknowledgements

Z.S. thanks the financial support from the National Natural Science Foundation of China (21671011), Beijing High Talent Program, and Beijing Natural Science Foundation (KZ201710005002). The authors thank China Postdoctoral Science Foundation and Beijing Postdoctoral Research Foundation. H.F. acknowledges partially support from the U.S. Department of Energy, Office of Basic Energy Sciences, Division of Materials Sciences and Engineering. Sandia National Laboratories is a multimission laboratory managed and operated by National Technology and Engineering Solutions of Sandia, LLC., a wholly owned subsidiary of Honeywell International, Inc., for the U.S. Department of Energy's National Nuclear Security Administration under contract DE-NA0003525. The authors thank China Postdoctoral Science Foundation, Beijing Postdoctoral Research Foundation and Dongguan Program for International S&T Cooperation (2015508102006).

Conflict of Interest

The authors declare no conflict of interest.

Keywords

carbon dots, effective conjugation length, light-emitting devices, multiple-color emission, phosphors

Received: August 20, 2017
Revised: September 28, 2017
Published online: November 27, 2017

[1] a) Q. Tang, W. Zhu, B. He, P. Yang, *ACS Nano* **2017**, *11*, 1540; b) X. Li, M. Rui, J. Song, Z. Shen, H. Zeng, *Adv. Funct. Mater.* **2015**, *25*, 4929; c) V. Gupta, N. Chaudhary, R. Srivastava, G. D. Sharma, R. Bhardwaj, S. Chand, *J. Am. Chem. Soc.* **2011**, *133*, 9960; d) X. Yan, X. Cui, B. Li, L.-S. Li, *Nano Lett.* **2010**, *10*, 1869; e) X. Yan, B. Li, L.-S. Li, *Acc. Chem. Res.* **2013**, *46*, 2254; f) Y. Li, Y. Hu, Y. Zhao, G. Shi, L. Deng, Y. Hou, L. Qu, *Adv. Mater.* **2011**, *23*, 776.

[2] a) H. Li, X. He, Z. Kang, H. Huang, Y. Liu, J. Liu, S. Lian, C. H. A. Tsang, X. Yang, S. T. Lee, *Angew. Chem., Int. Ed.* **2010**, *49*, 4430; b) J. Liu, Y. Liu, N. Liu, Y. Han, X. Zhang, H. Huang, Y. Lifshitz, S.-T. Lee, J. Zhong, Z. Kang, *Science* **2015**, *347*, 970; c) S. Zhuo, M. Shao, S.-T. Lee, *ACS Nano* **2012**, *6*, 1059; d) L. Cao, S. Sahu, P. Anilkumar, C. E. Bunker, J. Xu, K. A. S. Fernando, P. Wang, E. A. Guliants, K. N. Tackett, Y.-P. Sun, *J. Am. Chem. Soc.* **2011**, *133*, 4754; e) K. J. Williams, C. A. Nelson, X. Yan, L.-S. Li, X. Zhu, *ACS Nano* **2013**, *7*, 1388; f) H. Li, R. Liu, S. Lian, Y. Liu, H. Huang, Z. Kang, *Nanoscale* **2013**, *5*, 3289.

[3] a) L. Cao, X. Wang, M. J. Meziani, F. Lu, H. Wang, P. G. Luo, Y. Lin, B. A. Harruff, L. M. Veca, D. Murray, *J. Am. Chem. Soc.* **2007**, *129*, 11318; b) S. Zhu, Q. Meng, L. Wang, J. Zhang, Y. Song, H. Jin, K. Zhang, H. Sun, H. Wang, B. Yang, *Angew. Chem., Int. Ed.* **2013**, *52*, 3953; c) K. Hola, Y. Zhang, Y. Wang, E. P. Giannelis, R. Zboril, A. L. Rogach, *Nano Today* **2014**, *9*, 590; d) Y. Li, Y. Zhao, H. Cheng, Y. Hu, G. Shi, L. Dai, L. Qu, *J. Am. Chem. Soc.* **2012**, *134*, 15; e) Y. Song, S. Zhu, S. Xiang, X. Zhao, J. Zhang, H. Zhang, Y. Fu, B. Yang, *Nanoscale* **2014**, *6*, 4676; f) X. T. Zheng, A. Ananthanarayanan, K. Q. Luo, P. Chen, *Small* **2015**, *11*, 1620; g) S. Qu, X. Wang, Q. Lu, X. Liu, L. Wang, *Angew. Chem., Int. Ed.* **2012**, *51*, 12215.

[4] a) F. Wang, Y. Chen, C. Liu, D. Ma, *Chem. Commun.* **2011**, *47*, 3502; b) C. Sun, Y. Zhang, K. Sun, C. Reckmeier, T. Zhang, X. Zhang, J. Zhao, C. Wu, W. W. Yu, A. L. Rogach, *Nanoscale* **2015**, *7*, 12045; c) L.-H. Mao, W.-Q. Tang, Z.-Y. Deng, S.-S. Liu, C.-F. Wang, S. Chen, *Ind. Eng. Chem. Res.* **2014**, *53*, 6417; d) X. Guo, C.-F. Wang, Z.-Y. Yu, L. Chen, S. Chen, *Chem. Commun.* **2012**, *48*, 2692; e) F. Zhang, X. Feng, Y. Zhang, L. Yan, Y. Yang, X. Liu, *Nanoscale* **2016**, *8*, 8618; f) L. Mao, W. Tang, Z. Deng, S. Liu, C. Wang, S. Chen, *Ind. Eng. Chem. Res.* **2014**, *53*, 6417.

[5] X. Xu, R. Ray, Y. Gu, H. J. Ploehn, L. Gearheart, K. Raker, W. A. Scrivens, *J. Am. Chem. Soc.* **2004**, *126*, 12736.
[6] D. Qu, M. Zheng, L. Zhang, H. Zhao, Z. Xie, X. Jing, R. E. Haddad, H. Fan, Z. Sun, *Sci. Rep.* **2014**, *4*, 5294.
[7] X. Wang, L. Cao, S. Yang, F. Lu, M. J. Meziani, L. Tian, K. W. Sun, M. A. Bloodgood, Y. Sun, *Angew. Chem., Int. Ed.* **2010**, *49*, 5310.
[8] a) Y. Song, S. Zhu, S. Zhang, Y. Fu, L. Wang, X. Zhao, B. Yang, *J. Mater. Chem. C* **2015**, *3*, 5976; b) S. Zhu, X. Zhao, Y. Song, S. Lu, B. Yang, *Nano Today* **2016**, *11*, 128; c) S. Zhu, L. Wang, B. Li, Y. Song, X. Zhao, G. Zhang, S. Zhang, S. Lu, J. Zhang, H. Wang, H. Sun, B. Yang, *Carbon* **2014**, *77*, 462.
[9] J. Ge, Q. Jia, W. Liu, L. Guo, Q. Liu, M. Lan, H. Zhang, X. Meng, P. Wang, *Adv. Mater.* **2015**, *27*, 4169.
[10] a) D. Qu, Z. Sun, M. Zheng, J. Li, Y. Zhang, G. Zhang, H. Zhao, X. Liu, Z. Xie, *Adv. Opt. Mater.* **2015**, *3*, 360; b) X. Miao, X. Yan, D. Qu, D. Li, F. F. Tao, Z. Sun, *ACS Appl. Mater. Interfaces* **2017**, *9*, 18549.
[11] a) K. Jiang, S. Sun, L. Zhang, Y. Lu, A. Wu, C. Cai, H. Lin, *Angew. Chem., Int. Ed.* **2015**, *54*, 5360; b) S. Sun, L. Zhang, K. Jiang, A. Wu, H. Lin, *Chem. Mater.* **2016**, *28*, 8659.
[12] H. Ding, S.-B. Yu, J.-S. Wei, H.-M. Xiong, *ACS Nano* **2015**, *10*, 484.
[13] S. Lu, L. Sui, J. Liu, S. Zhu, A. Chen, M. Jin, B. Yang, *Adv. Mater.* **2017**, *29*, 1603443.
[14] a) G. Eda, Y.-Y. Lin, C. Mattevi, H. Yamaguchi, H.-A. Chen, I. S. Chen, C.-W. Chen, M. Chhowalla, *Adv. Mater.* **2010**, *22*, 505; b) M. A. Sk, A. Ananthanarayanan, L. Huang, K. H. Lim, P. Chen, *J. Mater. Chem. C* **2014**, *2*, 6954; c) D. Qu, M. Zheng, J. Li, Z. Xie, Z. Sun, *Light: Sci. Appl.* **2015**, *4*, e364; d) S. Qu, D. Zhou, D. Li, W. Ji, P. Jing, D. Han, L. Liu, H. Zeng, D. Shen, *Adv. Mater.* **2016**, *28*, 3516.
[15] S. N. Baker, G. A. Baker, *Angew. Chem., Int. Ed.* **2010**, *49*, 6726.
[16] Y. Chen, M. Zheng, Y. Xiao, H. Dong, H. Zhang, J. Zhuang, H. Hu, B. Lei, Y. Liu, *Adv. Mater.* **2016**, *28*, 312.
[17] D. Qu, M. Zheng, P. Du, Y. Zhou, L. Zhang, D. Li, H. Tan, Z. Zhao, Z. Xie, Z. Sun, *Nanoscale* **2013**, *5*, 12272.